Energy 282 (2023) 128397

Contents lists available at ScienceDirect

Energy

journal homepage: www.elsevier.com/locate/energy

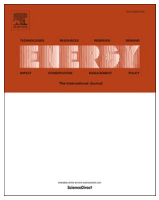

Dynamical modelling and experimental validation of a fast and accurate district heating thermo-hydraulic modular simulation tool

A. Dénarié *, M. Aprile, M. Motta

Department of Energy, Politecnico di Milano, 20156, Milano, Italy

ARTICLE INFO

Handling Editor: Henrik Lund

Keywords:
District heating
Modular modelling
Dynamic simulation
Validation
Monitoring data

ABSTRACT

This paper presents a new thermo-hydraulic model for district heating systems simulations, which aims at being a fast and accurate tool to simulate highly renewable networks characterized by fluctuating energy profiles. The main novel aspect of the tool lies in the heat transmission modelling over long pipes based on a Lagrangian numerical approach. In comparison to other existing models, this approach significantly reduces computational time and it increases results' accuracy. The elaborated method avoids numerical diffusion in the results and consequently allows proper prediction of temperature propagation, especially in case of fast changes of fluctuating profiles. The tool is built following a modular procedural programming approach in order to facilitate the simulation of multicomponent system. Thanks to its modular structure, every components of the system is built with the same structure that is differently declined according to each component's requirements. In this way, new additional elements' models easily fit the existing ones.

The model is validated under real operating conditions with hourly monitoring data of an Italian district heating network.

The results show good correspondence also in the most peripheral nodes of the network, where the largest deviations are normally encountered, thus making the model a reliable and fast simulation tool for district heating network design and operational control.

1. Introduction

District heating systems are energy infrastructures allowing the reduction of primary energy consumption [1] through the exploitation of local synergies between demand and available sources such as waste heat recovery and large use of renewable energies [2]. The exploitation of local renewable energy sources, especially in urban areas where free space is an issue, has brought to several projects of distributed integration of renewables and waste heat in existing and new DH systems [3–7]. In future energy systems, where heating and electrical sectors are strongly interconnected though DH [8], demand side management techniques and flexibility potentials strategies will be realized in DH systems especially in new generation ones such as 4GDH and 5GDH systems with distributed users located heat pumps [9].

Following this trend, DH networks are going to be more complex, with several generation systems distributed along the network and characterized by highly fluctuating energy profiles A detailed representation of temperature fluctuation propagations and pressure drops along these networks is therefore essential for both planning and operational optimisation. More specifically, it is desirable to evaluate, in each point of the network and over time, the variables that uniquely describe the status of the system: temperatures, flowrates and pressures. This to better forecast the performances of the distributed generation systems and their impacts on the network. Despite the well-known governing equations and the existing modelling approaches, the development of a fast and accurate DH simulation tool capable to predict the thermal and hydraulic behaviour of a DH network is not a trivial task that still needs further developments. Because of the large extension and the number of ramifications that usually characterize the DH systems, the effectiveness of thermal networks' modelling is still an open topic that the work here presented addresses: this paper presents a new thermo-hydraulic modular simulation model conceived for complex DH systems. The tool novelty lies in the inclusion of a pipe heat transmission model based on the Lagrangian method of characteristics. The approach, that has been presented and validated by the authors for one singe pipe in Ref. [10], is here integrated in a full simulation tool applied to a big scale DH system. In addition, the tool main advantage is that it' built with a modular procedural programming approach that facilitates the construction of multiple components models. The thermo-hydraulic full

* Corresponding author.
E-mail address: alice.denarie@polimi.it (A. Dénarié).

https://doi.org/10.1016/j.energy.2023.128397
Received 17 March 2023; Received in revised form 4 July 2023; Accepted 9 July 2023
Available online 11 July 2023

Abbreviations

DH	District Heating

Nomenclature

a	friction coefficient, m^{-2} kg^{-1}
C	linear heat capacity, J m^{-1} K^{-1}
F	force, N
h	linear heat transfer coefficient, W m^{-1} K^{-1}
L	pipe length, m
m	mass, kg
$\dot{m}$	mass flow rate, kg s^{-1}
p	pressure, Pa
$\dot{Q}$	heat, W
T	temperature, °C
t	time, s
v	fluid velocity, m s^{-1}
U	internal energy, W
$\dot{W}$	work, W
x	pipe section length, m

Greek symbols

θ	temperature, advection problem solution, °C
Δ	delta, difference

Subscripts

B	equivalent boundary layer (water boundary layer and steel pipe)
c	turbulent core
diss	dissipation losses
e	edge
el	electric
ext	external environment
gen	generation plant
i	pipe number
in	inlet
ins	insulation
loss	heat losses
n	node
out	outlet
w	water

model accuracy of the entire network is here investigated under real operating conditions by the comparison with yearly monitoring data of an Italian DH company located in the municipality of Lodi.

1.1. Existing models

The simulation of DH systems involves the description of both the hydraulic and thermal behaviours. The most commonly used mathematical model of thermo-hydraulic networks is the pseudo-dynamic [11], which has a steady-state formulation of the hydraulic problem and a dynamic solution of the thermal one.

1.1.1. Models of the hydraulic problem

The first approach to solve flow and pressures propagation over meshed network was developed by Hardy-Cross and it's based on the independent solution of each network loops by iteration. For a given pipe loop with known inlet and outlet flowrates, the unknown pipes' flowrates are calculated by an iteration process based on initially guessed flow values and a corrective factor. Flows' continuity equations at pipe nodes and pressures drops balances inside the loops are iterated until the corrective factor is zero. The Newton-Raphson method has been later used to solve water networks problems by applying it to pressure drops function. The method is matrix based, again iterative, but with multiple corrective factors, one for each flowrate value, and it's based on linear approximation of pressure drops functions.

In [12] the equations describing the hydraulic and dynamic thermal behaviour are solved simultaneously in a coupled Newton-Raphson power flow calculation. In Ref. [13] a new method to solve steady state hydraulics of complex networks is presented as more efficient an easier than the Hardy Cross method.

Some works include hydraulics dynamic behaviours in the modelling such as [14].

In [15] a DH model designed for multiple loops network is presented: the hydraulic problem is solved through the loop equation method, while the thermal one is solved with an upwind finite-difference method.

In [16] a method to solve both thermal and hydraulic problems of DH systems involving loops is presented. The model solves separately the transportation and the distribution networks to reduce computational costs; mass, momentum and energy conservation equations are written in a matrix form for all networks nodes. A similar model is applied in Ref. [17] to show how to exploit DH flexibility to shave peaks thanks to optimized flow rate control, while in Ref. [18] a model for the optimisation of meshed network is presented.

1.1.2. Models of the thermal problem

Several works dealing with the dynamical simulation of temperature propagation along the network have been found in literature and they are described in the following.

Simplifying approaches such as black box models [19] and aggregation methods [20] are useful to reduce simulation's time; nevertheless they are not adequate to study distributed energy connections in the networks since the connection with the network topology is lost.

Physical models, which explicitly describes the system's physical aspects, are preferred in this work application [15]. Heat transport physical models can be distinguished according to the method used to solve the advection problem; two main approaches can be identified: finite element and plug flow. Benonysson presents these two approaches in Ref. [11]: the *element method* is a finite difference method solving energy balance equations; the *node method* calculates pipes' temperature using time history of inflow temperature and mass flowrate being a version of plug flow approach.

Despite its great accuracy, the element method has two major drawbacks which affects its usability: the calculation time length and the occurrence of artificial numerical diffusion. Palsson [21] describes a different discretization scheme to be used in the element method, QUICK, intending to limit the numerical diffusion of upwind different scheme. Further work on finite difference modelling can be found in Refs. [22,23] where a new model of pre-insulated twin pipes is presented and in Ref. [15] where a model based on finite element is proposed to simulate networks with multiple meshes.

Concerning the node method, its strength is that, based on the plug flow approach, it only calculates incoming water segment propagation time and thermal losses. In this way, computational efforts are significantly smaller and artificial diffusion is avoided. The node method tracks the propagation time and the temperature value of all the water volumes travelling through the pipe. Nevertheless, its drawback can be found in the outlet result calculation that loses accuracy by mixing outlet volumes temperatures in a single value. Gabrielaitiene has given major contribution in analysing the node method performances thanks to several studies in comparing it with other modelling approaches [24], with commercial software TERMIS [25–27] and with monitoring data [28]. The outcome of these analyses is that the node method is faster and it doesn't' show numerical diffusion, but it presents inaccuracies in

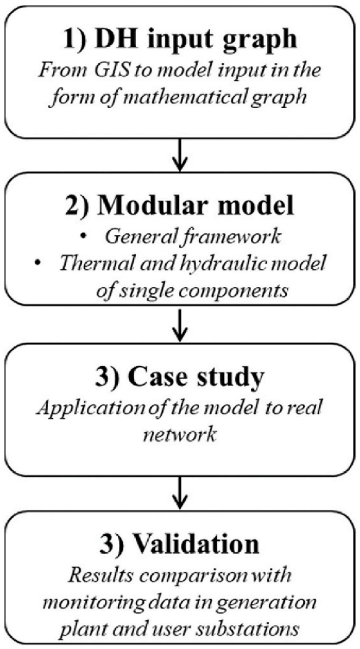

Fig. 1. Methodological steps.

distant point of the network with sharp temperature variations. Starting from the investigations of the node method inaccuracies, the authors of this work have developed a new Lagrangian numerical approach to simulate heat transmission in DH pipes by solving these issues. The pipe model presented in Ref. [10] is therefore here integrated in a full system model.

A similar approach is used in the pipe modelling of TRNSYS software [29]. An implementation of a Lagrangian approach to deal with the thermal simulation of piping network is presented in Ref. [30]: the author presents a district cooling network model emphasising the success of this modelling approach in particular with the elimination of numerical diffusion. A more recent paper [31] presents the comparison between the node method and the full implicit and Crank–Nicolson finite difference approaches: the results aim at helping future DH optimisation tool designers to choose an adequate pipeline model. In Ref. [32] a new model approach combining the features of plug-flow and discrete stirred tank includes the longitudinal dispersion of turbulent fluid, a novel aspect which is usually neglected, but that gain importance in low flow regime.

1.1.3. DH systems models

Using the presented approach, DH full system simulation tools have been found in existing works. An optimisation tool for DH network in Ref. [33] uses the pipe model presented in Ref. [10] as a planning tool for systems management. In Ref. [16] a full DH model for meshed network is presented based on finite elements approach.

In [34] a Lagrangian approach is used in a DH simulation tool: the tool focuses on the solution of the complex challenges of this numerical approach when a water segment has to traverse a highly branched network using recursive methods within the timestep. The tool has a particular accuracy in describing the mathematical approach and is rich in components variety, nevertheless is not validated under real operating conditions.

In recent year there has been a growing interest in using object-oriented modelling to simulate DH system. The plug flow approach has been preferred in this type of application: in Ref. [35], Giraud et al. present a Modelica library conceived to simulate DH networks and solar thermal integration; in Ref. [36], Van Der Heijde et al. show a Modelica software implementation of a thermo-hydraulic plug-flow model for thermal networks and validate it experimentally.

Following the purpose of open source models, some Python [37] based libraries have been built. DHNx [38,39] is the package inside the Oemof [40]optimisation framework that contains DH network optimisation and simulation models. In Ref. [41], DiGriPy, a newly developed Python tool for the simulation of DH networks based on the TESPy [42] package is presented.

Concerning the use of these models in real operational conditions, there's a general lack of works presenting validations based on long period measurements of real networks: in Ref. [28] the author presents an entire network validation for 2 winter days, in Ref. [27] 4 spring days are considered to validate a DH network, while in Ref. [43] a small DH network is validated during one winter day.

1.2. Motivation of the work

The analysis of existing models presented in the previous section highlights the advantages and limits of the most commonly used models based on finite element discretization. For these reasons the authors have chosen to developed a thermo-hydraulic model, which is here presented and investigated in its accuracy, with a novel modelling approach depending on the spatial extension of the system components.

The main strength of the work here described is represented by the modularity of the simulation tool, able to model complex system and flexible enough to choose the appropriate modelling approach for each component with the ambition to pursue a good compromise between simulation's accuracy and rapidity. The modular procedural programming approach used in the coding phase is particularly suitable for the modelling of multicomponent phase system. In fact, this programming syntax keeps the same common modelling framework for all the elements but it allows every component to be described by its own characteristic equations solved with different approaches.

The flexibility of the instrument is best expressed in the choice of the approaches to solve the thermal problem, different for each component. For all components that do not have a prevailing geometric dimension, a lumped capacity approach is used where the spatial discretization coincides with the single element. For the network pipes' model, the variable spatial discretization defined by the method of characteristics is chosen as presented by the author in Ref. [10]. In Ref. [10], the turbulent flow heat transmission model has been tested in a single pipe application: the results have shown that the temperature profile over long pipes is properly reproduced. Still, the benefits of this modelling approach can be fully appreciated only at the entire system scale, especially big scale system, which is instead shown in this paper. The aim of this paper is to show that the promising results presented in Ref. [10] for a single pipe are confirmed along the entire network together with the hydraulic behaviour prediction. The validation through the entire network modelling is particularly important in the Lagrangian approach because, differently from existing models, it allows the water volumes tracking though the entire network, in junctions and mixing points. The full model here presented allows fast simulations of big scale system with high quality accuracy especially in peripheral network points in case of rapid temperature variations.

After recalling the main assumptions and equations constituting the thermal and hydraulic models, the paper presents the comparison between the temperatures predicted by different simulations and their experimental counterparts.

2. Methodology

The aim of this work is to present the developed model and to validate its accuracy by applying it to a real DH network to simulate its behaviour. The main methodological steps are shown in Fig. 1 and described in the following.

First the geometry of the DH system, the network in particular, is taken from a GIS (Geographical Information System) file and converted

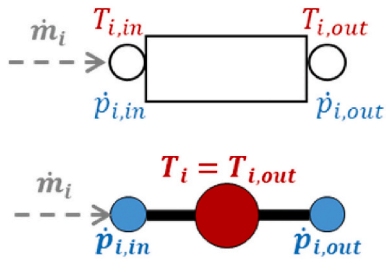

Fig. 2. Scheme of equivalent edge model: two blue hydraulic nodes and one single red thermal node.

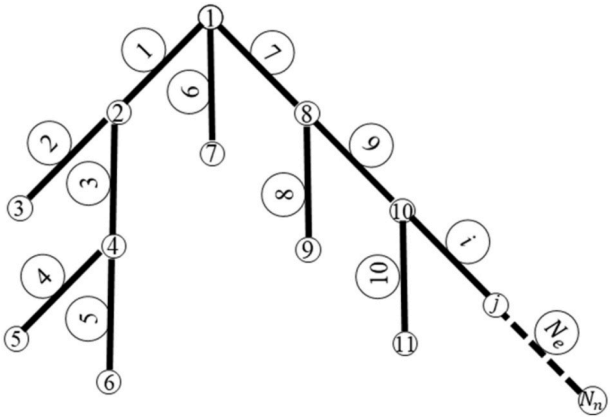

Fig. 3. Exemplification of the numbering of DFS algorithm.

in a mathematical graph as described in paragraph 2.1.1. The network graph is the input of the second step, the dynamical model, that is described in detailed in this chapter. The general modular modelling framework is developed and declined to every component's model to solve the hydraulic and thermal problem, solved in parallel, as described in 2.1.2, 2.2 and 2.3. The two available approaches to solve the thermal model, the lumped capacity upwind discretization and Lagrangian characteristics method, are described in 2.3. The Lagrangian approach implemented in this model can be used for tree shaped network only, for meshed network the lumped capacity upwind scheme is used. The model is written in Matlab and can be used to simulate city scale DH system with several users (in this case almost hundreds).

The built model is then applied to a real network in the north of Italy where a reference year has been used to simulate the hourly behaviour of the entire system. Finally the results of the simulations are compared to monitoring data in the main generation system, paragraph 3.2.2 and in user substations 3.2.1.

2.1. The model

This section describes the structure of the simulation tool and the mathematical model built to simulate pressure drops and temperature transient along the network. The main purpose of this modular simulation tool is the solution of the thermal and hydraulic problems characterizing the overall DH system that is here represented by a graph with edges and nodes. Each element's thermal and hydraulic behaviour is modelled through the equations of mass, momentum and energy conservation, declined differently for each component. The obtained outputs are the independent variables describing the system behaviour, in time t and space x in each i node of the network:

- Temperature $T_i(x,t)$.
- Pressure $p_i(x,t)$.
- Mass flowrate $\dot{m}_i(x,t)$.

The network is mathematically represented by a graph whose edges are the components constituting the system and the nodes represent the joints where the balance equations occur.

The model is based onto the following hypothesis:

- the water is considered as an incompressible and homogenous fluid;
- the material properties have constant values;
- the timestep is constant;
- the Lagrangian approach is used for pipes in tree shape network while finite difference is used for meshed network.

The model currently includes the following elements models that are described in detail in the Appendix:

- Pipe: main element of the distribution network that generates heat losses and pressure drops.
- Pump: element that increases the pressure in the system and covers the friction losses thanks to electrical consumption. Two types are available fixed and variable speed. It usually represents the main pumping sites in the central plant.
- Generation plant: heat producer with a certain efficiency responsible for keeping a certain set point of supply temperature.
- User substation: heat exchanger that represents the heat consumption at customers' substation causing a temperature reduction and pressure drop between supply and return line.

2.1.1. The network components' representation

The system is mathematically built as a graph where the components are modelled as edges connected by initial and final nodes. Every element has one lumped capacitance thermal node and two zero-capacity hydraulic nodes, characterized by their relative variables, temperature T_i and pressures p_i, as shown in Fig. 2.

The temperature of the edge is assimilated by its outlet node temperature. Every system's component is modelled by its constitutive equations: a unique modelling structure is however kept common for all the components to facilitate elements' connections following a procedural programming approach.

The network geometry input is built from the network GIS (Geographical Information System) shape file that is processed with a sequence of steps that connects edges and nodes and identify common nodes between edges. In particular, the application of the Depth-First Search algorithm [44], one of the most common graph algorithm, allows the subsequent numbering from the root point - the generation plant - towards the most peripheral points of the tree graph - the users. In this model, the supply and return line are symmetrical so the path is done backword for the return line. Fig. 3 shows the resulting numbering of the system elements. This ordered graph representation of the network is of particular importance since the solution of the distribution network heat propagation model is performed with a Lagrangian approach, so the order of the elements solution has an impact on the calculation.

The mathematical description of the entire system is therefore a graph composed by N_n nodes and N_e edges, where the edges are constituted by the network elements, such as pipes, pumps, heat exchangers, generation plant etc.; the nodes represent the points that connect the edges.

Two main structures are generated to contain all the information of system's geometry in order to solve the thermal and hydraulic network: the *edge-node* matrix and the *node-path* function. The *edge-node* $N_e \times N_n$ matrix contains 1, -1 or 0 if an edge flow is entering or leaving a node or it is not connected [16].

The node *node-path* function, built applying the Dijkstra's Shortest Path Algorithm between the node and the root node, describes, for every node, the sequence of all nodes crossed in the path to the generation plant. This function therefore creates the sequence of flow propagation

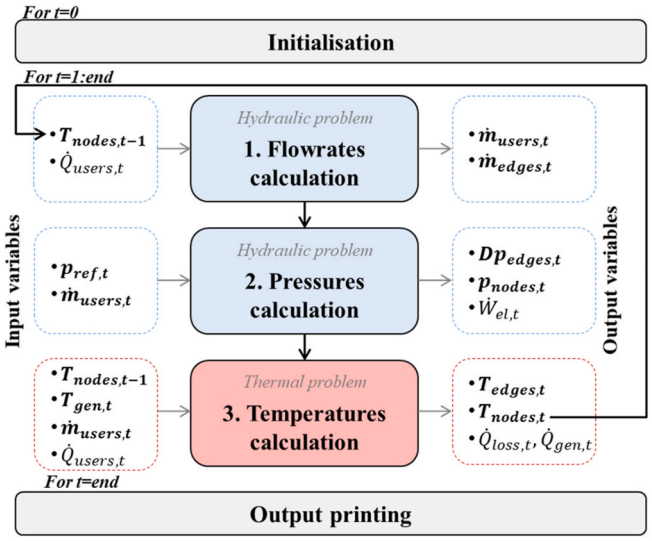

Fig. 4. Structure of model solution's steps.

from the generation plant to users' substations and back [15]. The flow propagation order defines therefore the elements simulation sequence of the thermal problem.

2.1.2. The model structure

A pseudo-dynamic solution method is used in this tool since the hydraulic problem is solved as steady state – hydraulic nodes has no capacitance-while the thermal problem incudes capacities and therefore dynamics. The appendix describes the detailed equations for every elements model.

Fig. 4 summarizes the main steps performed in the modelling tool to solve the entire system simulation that are afterwards detailed in the Appendix.

In each simulation time step, the hydraulic problem is solved with a steady-state approach, starting from the calculation of the flow rates $\dot{m}_{user,t}$ required at current timestep t at users' substations. In this step all flowrates $\dot{m}_i$ and pressures p_j of all edges i and nodes j are calculated along the network with the use of the *edge-node* matrix as described in section 2.1.1. Substations flowrates are determined with the customers required heat $\dot{Q}_{user,t}$ and with the supply temperatures to the heat exchangers $T_{nodes,t-1}$, being the latter calculated from the solution of the thermodynamic problem at the previous timestep. Within the time step when the thermal problem is solved, the flow rates are assumed to be constant. Thanks to the known flowrates in all the edges, the propagation of the input temperature from the generation plant $T_{gen,t}$ is calculated along the supply line of the network. Similarly, in the return line, the temperature profiles coming for the return temperature at user substations is propagated to the generation plant. The temperatures in all the points of the network $T_{edge,t}$ and $T_{node,t}$ are therefore calculated at the new timestep t in a dynamic way so including also previous timestep values as described in section 2.1.1. The new obtained temperature distribution allows the flow rates calculation in the following time step. An unavoidable time-lag of one-time step, due to the calculation method, is therefore maintained in the simulation. The appendix shows the details of the procedural approach used in every modelling step and the variables calculation.

2.2. The hydraulic problem

Pressures and flows' calculation is based on the mass and momentum continuity equation.

The mass conservation equation (2.1) is applied at every node to calculate the flowrate distribution along the network.

$$\sum_i m_i = 0 \tag{2.1}$$

The known terms are represented by the flowrate required at user substations which are usually known from monitoring results or calculated from users' consumptions. The inlet and outlet flows at every node are identified by the *edge-node* matrix. Once the flowrates are obtained, the steady state momentum balance equation is applied to all N_e edges to calculate pressure drops in pipes.

$$\frac{\partial p_i}{\partial x} + F_{fi} = 0 \tag{2.2}$$

Using the pipe length as spatial discretization in equation (2.2), the pressure drops can be calculated as:

$$\Delta p_i = -a_i L_i \dot{m}_i^2 \tag{2.3}$$

where a_i is the friction coefficient and L_i is the pipe length. The N_e equations (2.3) give the pressure distribution in the entire network from the pumping systems to the expansion vessel. The expansion vessel is considered as the reference node of the hydraulic circuit with an assigned pressure value.

In case of tree structured network, the system with N_n equations of mass continuity on nodes is determined. In case of meshed network with closed loop, the system is not determined. It is therefore necessary to add one additional equation for every mesh to obtain the mass flowing inside the loop: the sum of pressure drops inside the mesh should be equal to zero. To solve these additional equations, the Hardy Cross method has been used in this work.

2.3. The thermal problem: two solutions

The equation governing the problem is the conservation equation of energy (2.4):

$$\rho_i A_i c_{p,i} \frac{\partial T_i}{\partial t} + \rho_i A_i v_i c_{p,i} \frac{\partial T_i}{\partial x} + A_i v_i \frac{\partial p_i}{\partial x} + \dot{Q}_i + \dot{W}_i = 0 \tag{2.4}$$

The equation represents the energy balance over the cross sectional area, so expressed in a linear form: the rate of change of the energy stored in the water section A is equal to the flux of enthalpy crossing the element and the heat $\dot{Q}$ and the electrical work $\dot{W}$ entering the element. (e.g. heat supplied by the generator in the boiler model, electrical input in the pump model, etc.). The solution of the energy balance equation in the thermal problem allows obtaining the variable $T_i(x, t)$. Two numerical approaches are here used to solve the thermal problem: the lumped capacity method for punctual elements and the method of characteristics for pipes. The "punctual" components are the ones for which parameters describing them do not change over the longitudinal direction such as pumps, heat exchangers and generation systems.

2.3.1. The lumped capacity method

According to the lumped capacity method, the elements are modelled as a single node with the entire capacity concentrated in one single point and uniform temperature. The hypothesis of temperature uniformity allows substituting the temperature spatial derivative with the temperature difference between input and output in the energy balance. Using an upwind discretization scheme, all the capacity is lumped at the outlet section of the element. In this way, the element i temperature difference between inlet and outlet becomes the temperature difference between element i and the previous i-1.

$$\frac{dT_i}{dx} = \frac{(T_{i,in} - T_{i,out})}{\Delta x} = \frac{(T_{i-1} - T_i)}{L_i} \tag{2.5}$$

Consequently, for elements' thermal node, equation (2.4) becomes:

$$\rho_i A_i c_{p,i} \frac{\partial T_i}{\partial t} = \dot{m}_i c_{p,i} \frac{(T_{i-1} - T_i)}{L_i} + A_i v_i \frac{(p_{i-1} - p_i)}{L_i} + Q_i + W_i \tag{2.6}$$

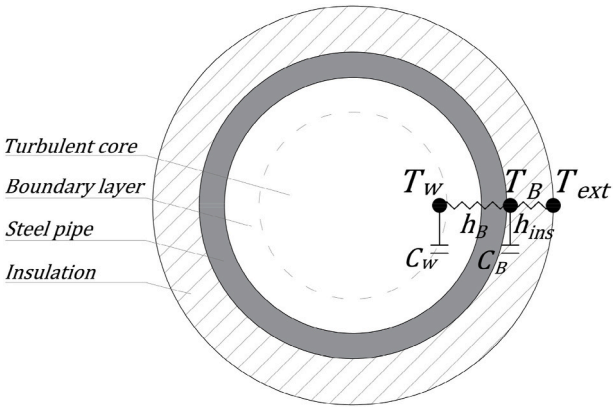

Fig. 5. Two nodes model of heat transmission in water pipe.

2.3.2. The characteristics method

The heat transmission over distribution pipes has been modelled with a new numerical approach [10] based on characteristics method [45]. The detailed description of the method can be found in Ref. [10] and it is here summarized. The model includes also the turbulent flow characteristics therefore the energy balance equation applied to the pipe is split between the water core and the boundary steel pipe including the boundary water layer. The energy balance equation (2.4) applied to the network pipes is split in the system (2.7):

$$\begin{cases} \dfrac{\partial T_w}{\partial t} + v\dfrac{\partial T_w}{\partial x} + \dfrac{h_B}{C_w}(T_w - T_B) = 0 \\ \dfrac{\partial T_B}{\partial t} + \dfrac{h_B}{C_B}(T_B - T_w) + \dfrac{h_{ins}}{C_B}(T_B - T_{ext}) = 0 \end{cases} \tag{2.7}$$

The first equation is the energy balance for turbulent water core; the second is for a boundary layer including water viscous and diffusive layer and the steel pipe, as Fig. 5 shows. The thickness of the sublayer and its linear heat transfer h are calculated according to Gnielinski formulation [46].

The mathematical approach used to solve the system is the splitting approach [47] which consists in splitting the system in the advection problem (2.8) and the source problem (2.10)

$$\begin{cases} \dfrac{\partial \theta_w}{\partial t} + v\dfrac{\partial \theta_w}{\partial x} = 0 \\ \theta_w(x, t_0) = T_{w0}(x) \end{cases} \tag{2.8}$$

The advection problem is solved with characteristics method for which

$$\theta_w = T_w(x_0) = T_w(x - v\,\Delta t) \tag{2.9}$$

Boundary layer' thermal capacity and heat losses effects are accounted for by solving the source problem:

$$\begin{bmatrix} \dfrac{dT_w}{dt} \\ \dfrac{dT_B}{dt} \end{bmatrix} = \begin{bmatrix} -\dfrac{h_B}{C_w} & \dfrac{h_B}{C_w} \\ \dfrac{h_B}{C_B} & -\dfrac{h_B + h_{ins}}{C_B} \end{bmatrix} \begin{bmatrix} T_w \\ T_B \end{bmatrix} + \begin{bmatrix} 0 \\ \dfrac{h_{ins}}{C_B} T_{ext} \end{bmatrix}$$

$$\begin{matrix} T_w(x, 0) = \theta_w(x, t) \\ T_B(x, 0) = \theta_B(x, t) \end{matrix} \tag{2.10}$$

where T_w is the temperature of the water turbulent core and T_B is the temperature of the boundary layer. The system is analytically solved by being in the form of ordinary differential equation $\frac{dT}{dt} = [A]\,T + b$. Following the Lagrangian approach, the solution order of pipes' equations is defined by the *node-path* function presented in 2.1.1.

3. The case study

The installation of Lodi district heating dates to 2004 and, at the end

Table 1
Uncertainty of measurement data.

Position	Measure	Tool	Error	Unit
Substation	Flow rate	Ultrasonic flowmeter	$\pm\left(2 + 0.02 \bullet \frac{\dot{m}_{nominal}}{\dot{m}}\right)$	%
Substation	Temperature	Pt 500	$\pm\left(0.5 + 3 \bullet \frac{\Delta T_{min}}{\Delta T}\right)$	%
Central plant	Flow rate	Magnetic flowmeter	$\pm(0.5 \bullet \dot{m})$	%
Central plant	Temperature	Pt 500	$\pm(0.3 + 0.005 \bullet T)$	[°C]

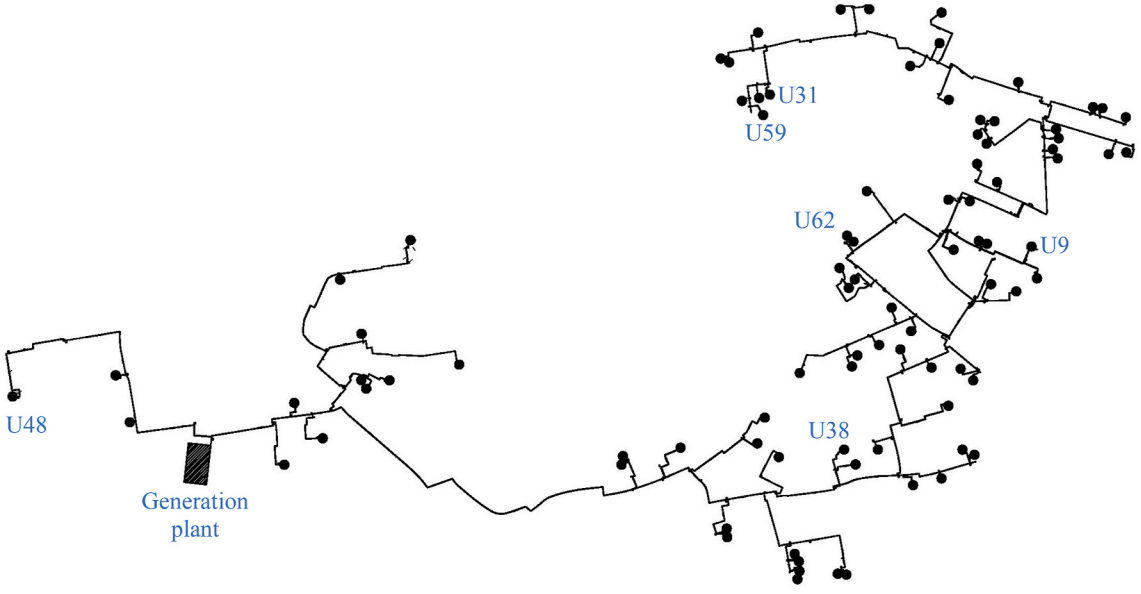

Fig. 6. Lodi district heating system network in 2013.

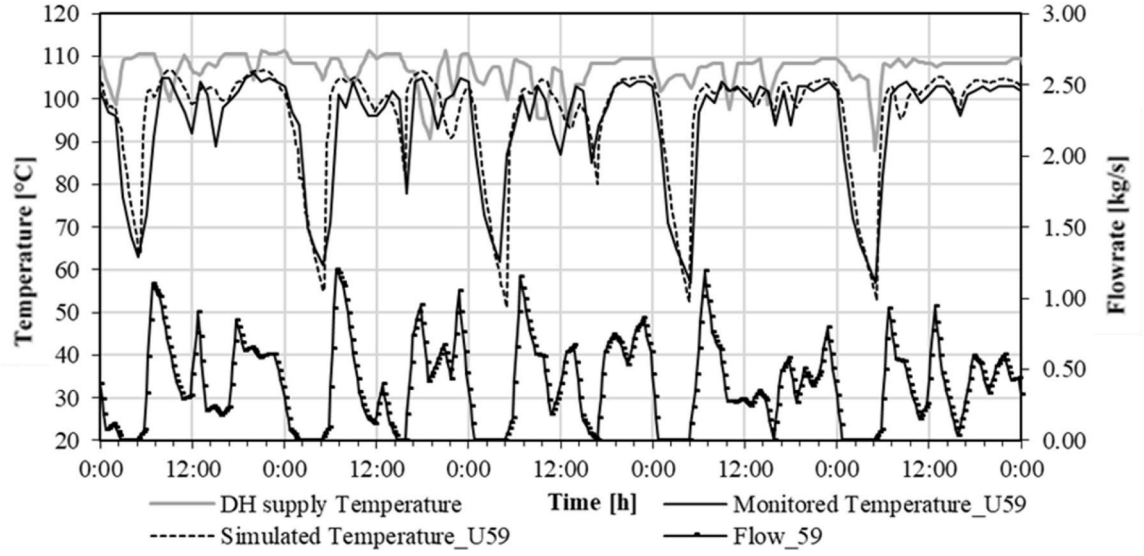

Fig. 7. Supply temperature and flow rate for user 59 – residential - December.

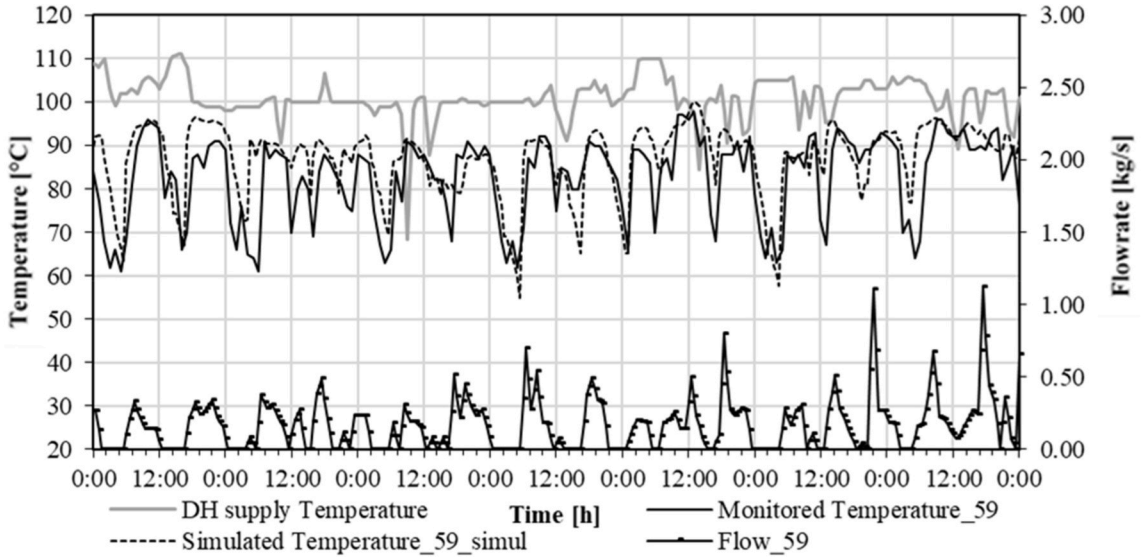

Fig. 8. Supply temperature and flow rate for user 59 – residential - October.

Table 2
User supply temperature: average error and its standard deviation, root mean square error related to user location.

		December		*October*	
User	Distance [m]	Av. error [°C]	St. dev. [°C]	Av. error [°C]	St. dev. [°C]
59	4405	0.12	1.60	−0.44	6.30
64	1017	0.18	2.91	−0.05	3.46
62	2811	0.09	1.55	0.39	4.62
31	4302	0.16	1.51	0.06	5.71
48	941	0.05	2.68	−0.14	3.27
38	1863	0.02	1.55	−1.33	5.51

of 2012, 90 users were connected, corresponding to 1 267 600 m^3 of building volumes (approximately 10 000 inhabitants). Out of this volume, 560 600 m^3 is the share of residential buildings while 707 000 m^3 represents administrative, commercial and tertiary users. The generation park at this date consists of a natural gas cogeneration plant with a capacity of 3.86 MW_{el} and 3.83 MW_{th} and 29 MW_{th} of natural gas back up boilers. The renewable share of thermal production is given by the heat recovery from a third party biomass ORC [48]. An important extension project has started in 2014 which implies approximately 30 new substations per year till the end of 2018, reaching 200 users. In this work the system is analysed in the configuration of 2013 before the extension. DH provides 36.7 GWh of heat, of which the 16% is represented by heat losses. The heating season lasts from mid-October to mid-April. During summer, the system delivers heat only to produce domestic hot water which represents the 14% of the total heat production over the year. DH consumers to whom heat is delivered heat for DHW production usually have centralized distribution system with storage tanks, instead of producing DHW instantaneously; this leads to a quite flat load profile for DH systems in summer time. The winter months, on the contrary, are characterized by a much more variable profile: space heating systems are generally radiators which are regulated with night set-back and intermittent operation during the day. This leads to a fluctuating demand profile with pronounced peaks.

A 600 m^3 storage tank helps reducing peak demands at the

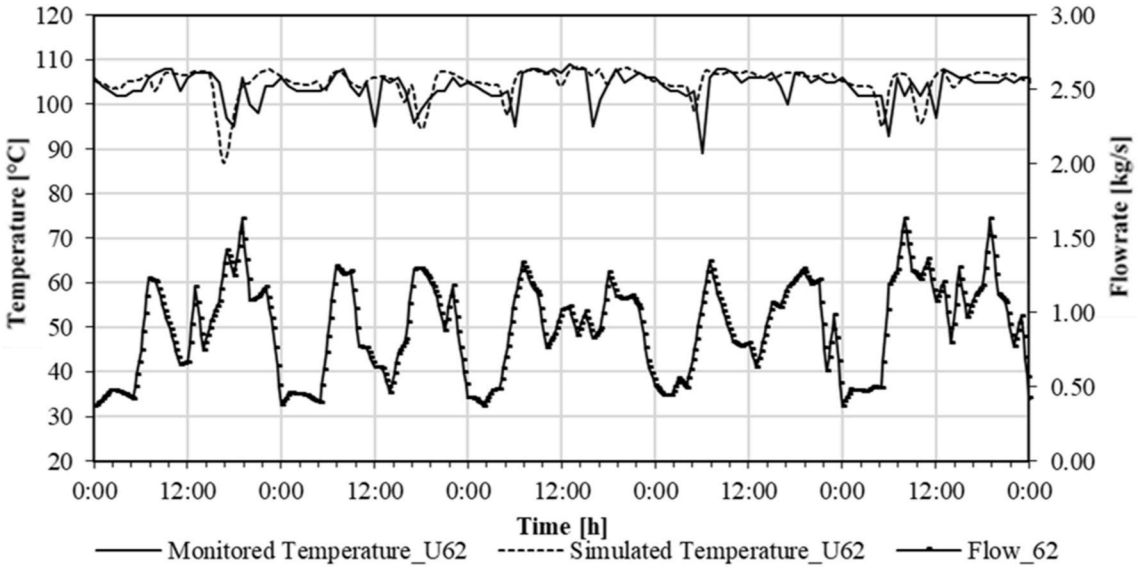

Fig. 9. Supply temperature and flow rate for user 62 – residential – December.

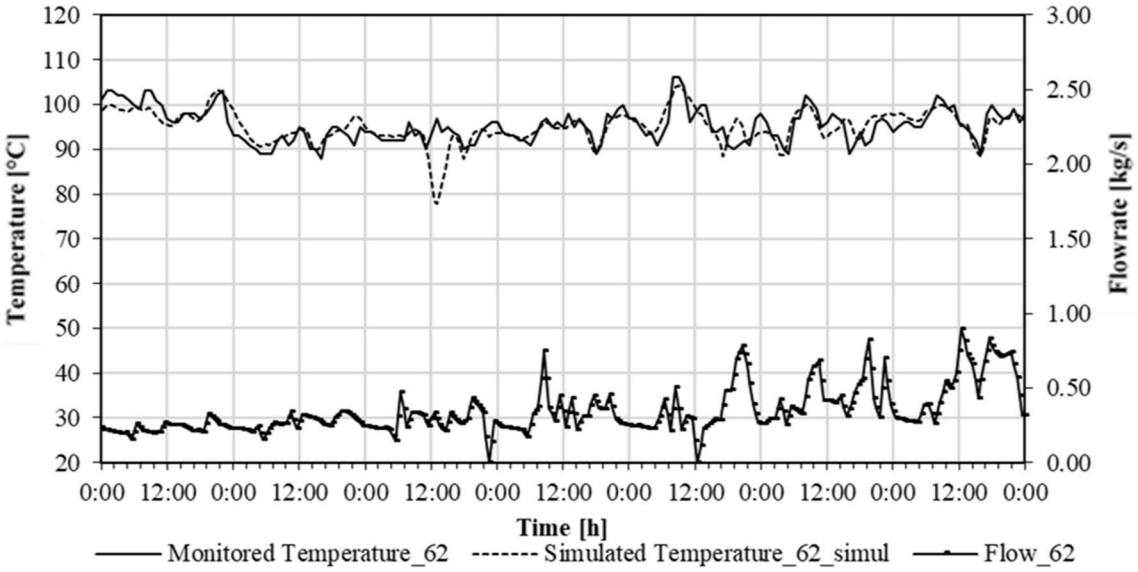

Fig. 10. Supply temperature and flow rate for user 62 - residential - October.

generation plant and it allows a better management of the generation systems. Fig. 6 shows the district heating system: the distribution network is 15 km long and it is made of pre-insulated pipes ranging in diameter from 32 to 300 mm.

Consumers are connected through flat plate heat exchangers: the primary side of the substation is regulated by a control system which reacts to consumer behaviour to guarantee temperature set points on the secondary side.

The main effect of user energy demand is a variation in flow rate and return temperature on the substation; on the heat generation side, the DH supply temperature is set in order to supply enough energy to all consumers.

3.1. Measurement data

Monitoring data used in this study includes temperatures, flowrates and energy delivered on the primary side of users' substations as well as supply temperature from the generation plant. Data were collected with 1-h time step along the year by the remote data logging systems installed on the substations. The generation plant data logger instead records data every four days a week in the heating season, from October to March. The uncertainties related to measurement tools are shown in Table 1.

Simulations' results have been analysed to validate the model ability to properly predicts network dynamics. The comparison between model outcomes and monitoring data has been done at the inlet of users' substations, to check supply temperatures to consumers, and at the generation plant, to check the overall network return temperature. Particular attention has been given to this last value and to peripheral users' supply temperatures since the main outcome from previous studies about existing models [26] is that the discrepancies between the predicted and measured temperatures are bigger for distant consumers.

For winter regime, five days of December (9th to 14th) have been analysed, while for mid-season regime, with low space heat demand, the last days of October (21st to 28th) have been considered.

For yearly performances validation, the simulated total heat production and heat losses are compared with monitoring data given by the

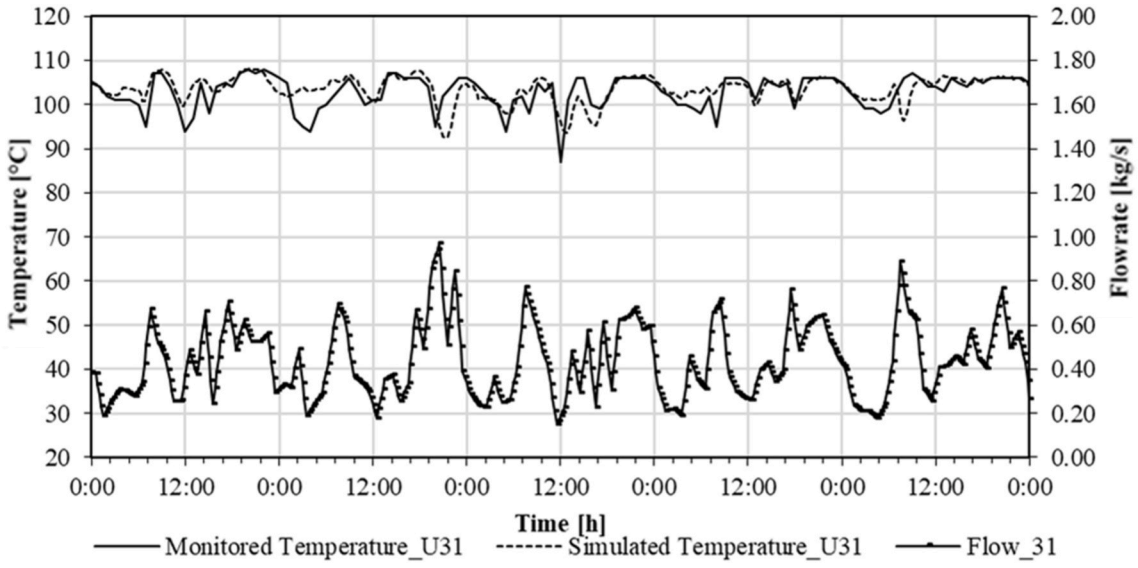

Fig. 11. Supply temperature and flow rate for user 31 – residential - December.

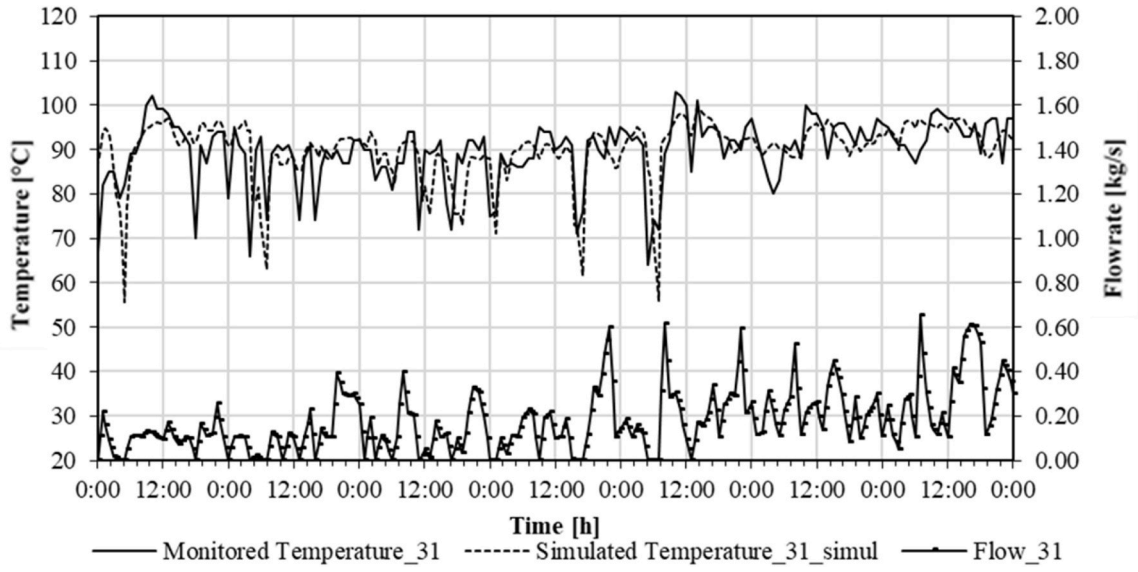

Fig. 12. Supply temperature and flow rate for user 31 – residential - October.

DH company.

3.2. Simulation results

In this section the results of the dynamic simulation of the entire system are presented and compared to monitoring data in order to validate the model. Specific attention is given to the temperature propagation in the network in terms of the value of the temperature but also of the timely profile. To do this, the variables requiring specific analysis are the simulated temperatures at the furthest points from the input data: namely the supply temperatures at the users' substations to verify the propagation on the supply line and the return temperature at the main generation plant to verify the results on the return line.

With regard to the first point, the average error and the mean square deviation of the supply temperatures at the users' substations are presented in 3.2.1. First some significant substations, marked on the map of Fig. 1, are analysed in detail and then the error trend of all substations is reported in Fig. 17 in relation to their distance from the central plant station. This aspect in particular is emphasised since one of the literature review outcome is that the simulation error increase with the distance from the input point. The aim here is to show that the developed model neither amplifies nor propagates the error along the network. In a specular way, the propagation of the error on the return line is shown to be avoided by verifying the simulation result with the monitoring of the network return temperature at the generation plant in paragraph 3.2.2. The overall DH system simulation results in terms of energy, e.g. annual production, heat losses and electrical consumptions for the circulation pumps, are finally illustrated in comparison with the monitoring data in paragraph 3.2.2 to validate the overall model of the entire system in terms of consumptions.

3.2.1. Substations supply temperature

Supply temperatures at user substations are here presented comparing simulation results to monitoring data. Fig. 6 shows the analysed users: they are located in peripheral nodes of the network, they have different load profiles and they serve buildings with different use. They have been chosen to test the model validity with respect to temperature propagation along the network with fluctuating water flows

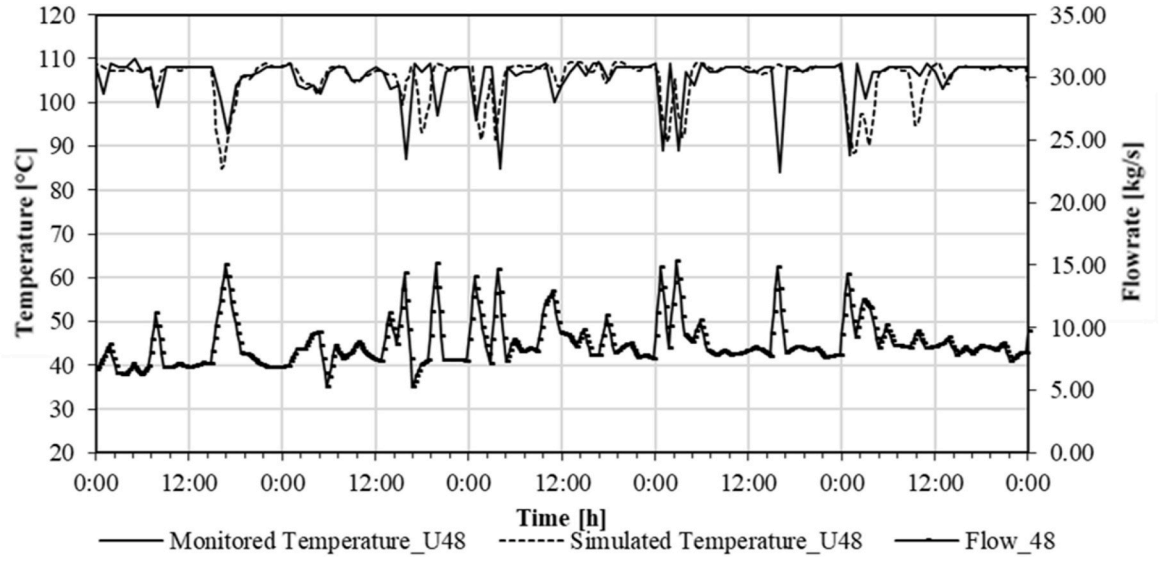

Fig. 13. Supply temperature and flow rate for user 48 – educational - December.

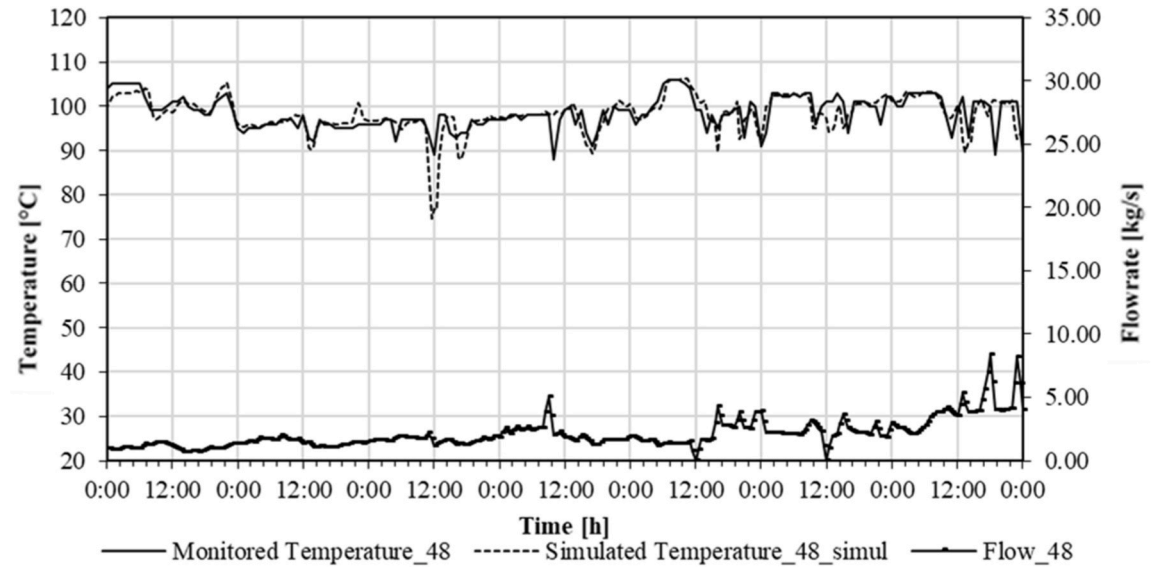

Fig. 14. Supply temperature and flow rate for user 48 – educational - October.

and input temperatures. Figs. 7–16 show the results from the selected users and Table 2 summarizes the differences between modelled and monitored temperatures as a function of the distance from the generation plant.

Looking at simulations outputs, it can be noticed that the model results are in substantial agreement with monitored data for all load types and without particular influence of the substation distance on the deviations. User 59 is a residential building with the typical flow profile characterizing residential heat demand in Italy. Night setbacks with the consequent important morning peaks demand clearly stand out from Fig. 7. The model proves to satisfactorily simulate the temperature propagation as well as the evening temperature drop and the fast and wide increase after the morning switch on. It's worth noticing that user 59 is the most distant from the generation plant: temperature wave has not been smoothened and transmission time is respected.

Consumers 62 and 31 (Fig. 9-Figure 10 and Figure 11-Fig. 12) have a quite irregular load demand with important fluctuations during the day, with no night set back.

Consumer 31 is located close to 59 so in the most peripheral area of the DH system; user 62 is located in the area of the system in which the network is meshed. The validation of the model in this point allows validation of the hydraulic solution of the meshed network.

User 48 is the last consumer on the left branch of the network and it's also the biggest user with an annual heat load corresponding to 11% of the total DH heat demand. Finally, Fig. 15 and Fig. 16 show results for consumer 38: this user has an almost constant flowrate which allows validating the propagation phenomena from generation plant alone without the influence of user dynamics.

Table 2 summarizes supply temperature's average errors and their standard deviations for all the presented users. The table includes also the users' distance from generation plant. No particular correlation between the error and the user location can be observed: neither on the average error, neither on its standard deviation.

Table 2 summarizes the error in simulating the supply temperature for the selected users presented in the previous section. The same results but for the entire set of network's users are calculated and presented in a graphical form in Fig. 17. It appears that neither the average errors neither its standard deviation increase with the distance from the

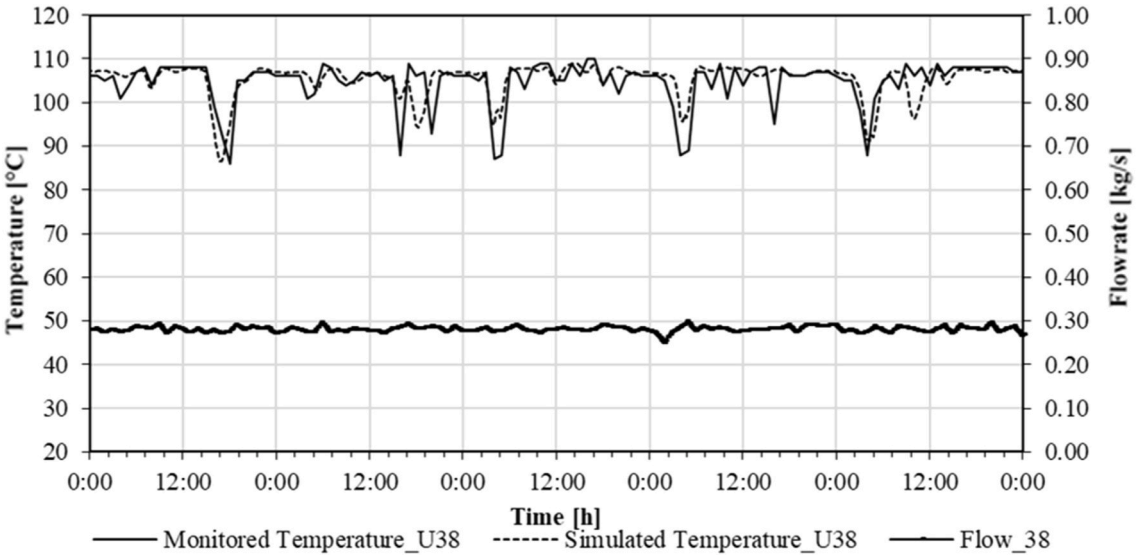

Fig. 15. Supply temperature and flow rate for user 38 – health - December.

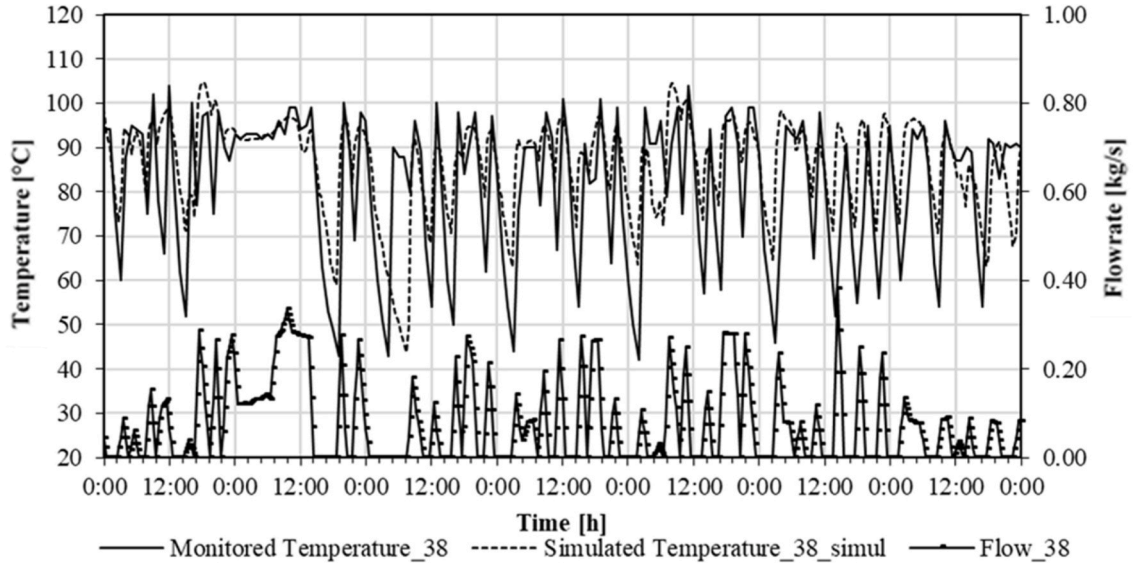

Fig. 16. Supply temperature and flow rate for user 38 - health - October.

generation plant. The average errors between monitored and simulated supply temperatures are due to incorrect estimation of the heat loss. There are many factors for this: the aging of the insulation which can vary the heat conductivity of pipes, non-uniform soil, the lack of insulation in some pipes or part of it, a certain inaccuracy in estimating the ground temperature. A deeper investigation on single aspects and components characteristics would reduce this error by better calibrating heat loss coefficients. The average errors do not measure the ability of the model to simulate temperature dynamics, which is instead evaluated by the standard deviation. Bigger errors can be noticed in October simulation. This can be explained by the monitoring data quality. In this period, heat demand and, consequently, flow rate are small, thus the measurements are affected by a larger uncertainty. The cause of bigger standard deviation errors can be the monitoring data logging time. In fact, in this period, frequent turning on and off can be noticed. Even if simulation time step is smaller, monitoring data are taken instantaneously every hour and linearly interpolated. This can cause an artificial time lag in the comparison of result. The level of accuracy of monitored data cannot give a sure explanation, these considerations remains possible reasons according to the authors. A more frequent and accurate monitoring system would be required to further analyse the cause of these errors.

3.2.2. Return temperature and energy production of generation plant

The return temperature at generation plant predicted by simulation is presented in Fig. 18, along with temperature and flowrate monitored data. Five, non-consecutive, days have been analysed. The model output profile is very close to the real one: the average error over the five days is −0.1 °C while its standard deviation is 1.12 °C.

As for comparison at user's substations, the propagation time is satisfactorily simulated, especially considering that the monitoring data frequency is 1 h. The morning peak demand, which here corresponds to the moments in which the return temperature has the minimum value, is the most critical day event for the generation plant: the model shows to predict it in an accurate way, considering both time correspondence and temperature values. The difference between predicted temperatures and the monitored ones is not uniform. The biggest discrepancies can be noticed in the very first hours of the day. In particular, on the 17th and

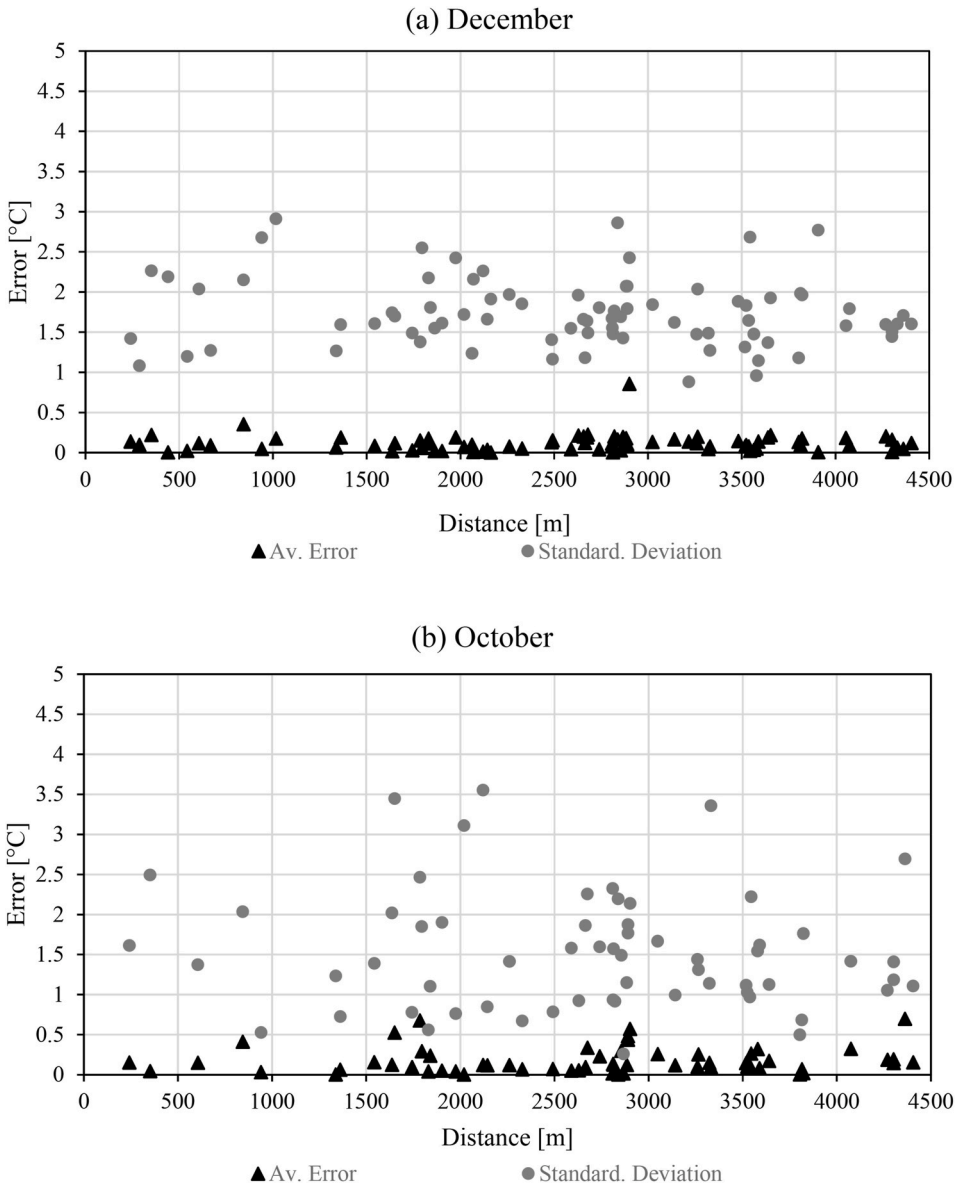

Fig. 17. Correlation between supply temperature errors and user location in the network in December (a) and in October (b).

the 21st of December, the simulated temperatures are higher than monitored ones; the lack of monitoring data in the previous time steps makes further investigations difficult.

Finally, the results of one-year simulation are presented in Table 3: the forecasted values come out being very close to energy production data given by the utility. Simulation time of the entire network composed by 485 edges is 2 h and 7 min (Processor i-5 CPU 2.5 GHz).

Once the model is validated with monitoring data, it's worth comparing its performances with the other existing methods to see if all this work has been worth.

Fig. 19 shows the difference between the new model results and a finite volume method with lumped thermal capacity (FVM with) different discretization mesh in time and space: the picture highlights the artificial diffusion which characterizes the discretization of FVM and it shows how the new approach produces results which are closer to monitoring data. Considering yearly energy results, the FVM with the same simulation time step, dt = 0.25 h, produces results with 3% and 0.5% errors respectively on heat losses and heat production, so generally bigger than the ones shown in Table 3. But most of all the difference lies in the inaccurate time delay which the FVM shows in Fig. 19 and in simulation time as Table 4 shows.

4. Discussions and conclusions

In this work the accuracy of a new modelling tool to simulate DH systems is investigated. The strength of the simulation tool lies in the flexibility of the modelling approach that can be chosen for each component in order to have better accuracy and lowest computational effort. The modularity of the model makes it suitable to simulate multicomponent systems such as city scale DH. The inclusion of the Lagrangian approach to model the network increases significantly the accuracy of the final results, avoiding the numerical diffusion effects still noticeable in existing models and reducing the simulation time. Nevertheless, the limit of this approach is that, in the current configuration, it can be used only for tree shaped network where the flow directions are known a-priori.

This work joins the list of few DH modelling tools that have been fully validated at system level with monitoring data. The monitoring data of a DH system in northern Italy have been used here to validate the presented model. The most important validation step is the comparison

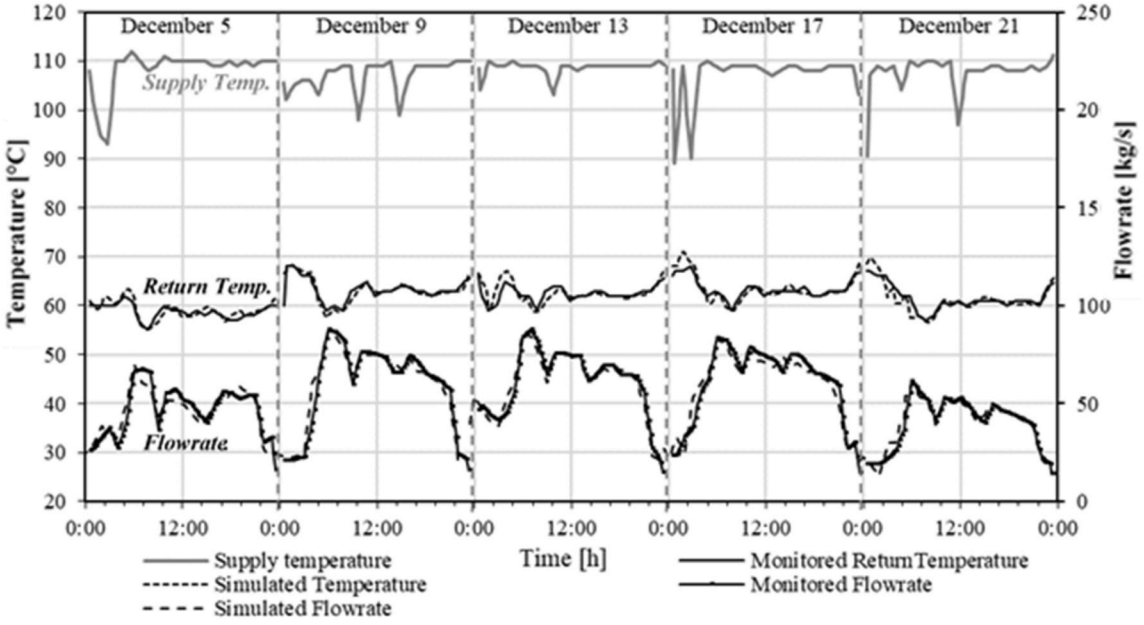

Fig. 18. Return temperature and flow rate at the generation plant – December.

Table 3
Comparison between simulation and real measured heat losses and energy production at generation plant.

	Heat losses [MWh]	Heat production [MWh]
Simulation	5710	36 642
Monitoring	5832	36 769
Error	−2.1%	−0.3%

of its performances with real DH network monitoring data. This test is difficult to carry out because the quality of collected data in such a big and complex systems is often non satisfactory: monitoring data are often incomplete, monitoring devices are sometimes defective at user sub-stations as well as at the generation plants or data logging works improperly.

A general problem is the inaccuracy of flow meters at very low loads which leads to bigger inaccuracies in mid-season and summer.

The validation of the model has been done accordingly to monitored data quality,: a certain degree of uncertainty still remains but the overall results are satisfactory. Especially results at distant points of the network show good correspondence to monitoring data and the model shows to properly forecast the peak in the central generation plant.

Looking at the validation outcomes, the model can be considered appropriate to make realistic assessments of the network behaviour in the presence of hypothetical structural changes, such as new branches or peripheral generators, in order to assess its economic convenience.

Considering its currents use, for validation or network optimisation's purposes, the model needs to be fed by a significant quantity of

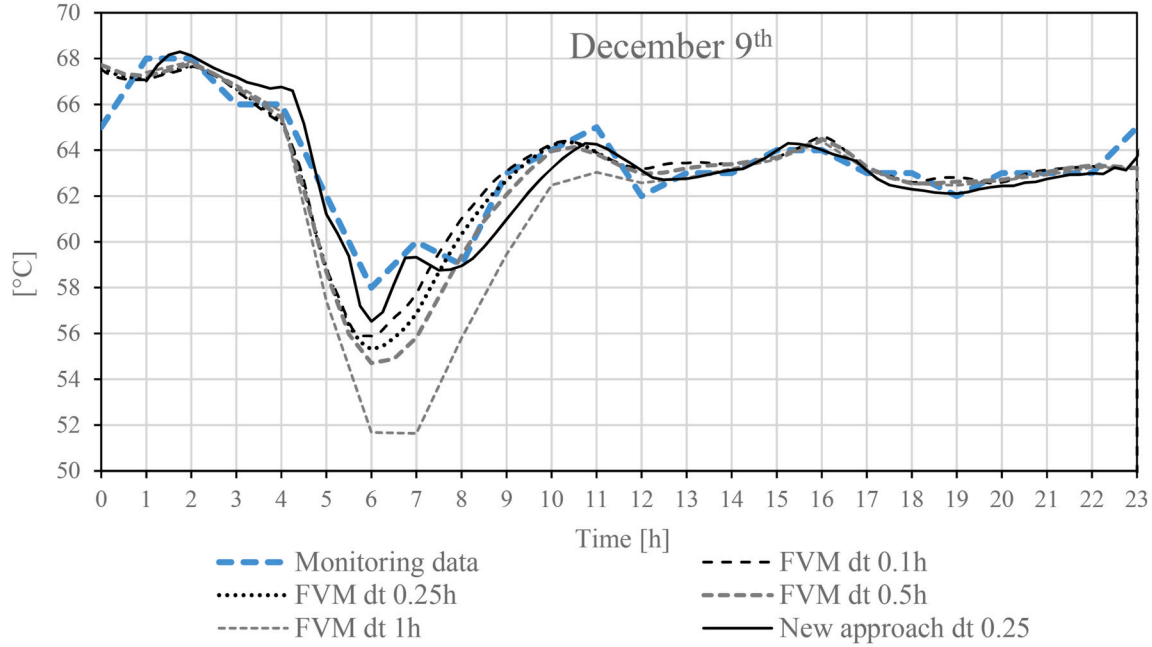

Fig. 19. Return temperature at the generation plant FVM vs New approach simulation results –December 9th.

Table 4
Comparison between FVM and the developed method performances.

	Simulation	New method (dt = 0.25 h)	FVM (dt = 0.25 h)
Simulation time [s]	December 9th	4.04 s	416 s
Standard deviation on return temperature [°C]	December 9th	−0.3	−0.4
Average error on return temperature [°C]	December 9th	0.6	1.5
Error on heat losses	Entire year	−2.1%	3%
Error on heat production	Entire year	−0.3%	5%

monitoring input data in all users' substations, with all the problems previously mentioned.

A general problem of lack of good quality monitoring data in big systems is identified, especially for the hydraulic system behaviour. Nevertheless, dynamic simulation tools can be used exactly for this purpose so to predict the system's performances in all the points with no measurement devices.

Future development of the model incudes the development of the Lagrangian approach for meshed networks and the estimation of user substations' behaviour in order to reduce the need of monitoring data.

Credit authorship contribution statement

Alice Dénarié: Conceptualization, Methodology, Software, Writing – original draft, Writing – review & editing. **Marcello Aprile:** Conceptualization, Methodology, Software, Writing - Review & Editing. **Mario Motta:** Supervision, Project administration, Funding acquisition.

Declaration of competing interest

The authors declare that they have no known competing financial interests or personal relationships that could have appeared to influence the work reported in this paper.

Data availability

The data that has been used is confidential.

Acknowledgements

The authors gratefully acknowledge Lodi Linea Green Gruppo A2A for providing monitoring data of the network.

Appendix

In this section the structure of the model describing the elements composing the network is described. The different elements' models are defined as Types. The type model is composed by equations and parameters set up functions grouped in cases which are called at every timestep.

General structure of the type

Case 1. – Initialisation of the variables

Case 2. – Inputs: read external files, parameters and previous steps results (+ calculation of substation flowrates in user type)

Case 3. – Hydraulic problem: flowrates $\dot{m}$, pressures p and dissipation losses calculations $\dot{Q}_{diss}$

Case 4. – Thermal problem: temperatures T, heat losses $\dot{Q}_{loss}$, internal energy change ΔU calculations

Case 5. – Energy balance components (outputs): Work input and output, heat input and output, heat generation, heat losses and internal energy change calculations

Solution steps of the types

Following the simulation steps of the model presented in Fig. 4, here the functional programming approach is described. For every step the suitable cases are recalled.

Table 4.1
Simulation steps and relative cases and calculates state variables and outputs

Simulation step	Case	Types				Nodes
		Pipe	Pump	User	Generation	
Initialisation	**1**	T_{in}, L	T_{in}	T_{in}	T_{in}	T_{nodes} **- energy conservation**
	2	T_{ext}		$\dot{Q}_{user}$, $\dot{m}_{user}$	T_{gen}	
Flowrates calculation	**3**	$\dot{m}$	$\dot{m}$		$\dot{m}$	**Mass conservation**
Pressures calculation	**3**	p, $\dot{Q}_{diss}$	p, $\dot{Q}_{diss}$	p, $\dot{Q}_{diss}$	p, $\dot{Q}_{diss}$	**Momentum conservation**
Temperatures calculations	**4**	T, $\dot{Q}_{loss}$	T, $\dot{Q}_{loss}$, ΔU	T, $\dot{Q}_{loss}$, ΔU	T, $\dot{Q}_{loss}$, ΔU	
Outputs	**5**	$\dot{Q}_{loss}$, ΔU, $\dot{Q}_{diss}$	$\dot{Q}_{loss}$, ΔU, $\dot{Q}_{diss}$, $\dot{W}_{in}$	$\dot{Q}_{user}$, $\dot{Q}_{diss}$	$\dot{Q}_{gen}$, ΔU, $\dot{W}_{in}$	

Model equations of the types

Pump

Hydraulic curve	$\Delta p = d\,\Delta p_{max}\left(1 + k_1\left\lvert\frac{\dot{m}}{\dot{m}_{max}}\right\rvert - (1 + k_1)\left\lvert\frac{m}{\dot{m}_{max}}\right\rvert^2\right)$
Momentum	$p_{out} - p_{in} = \Delta p - a\,L\,\lvert\dot{m}\rvert\dot{m}$
Efficiency curve	$\eta = e_0 + e_1\left(\frac{\dot{m}}{\dot{m}_{max}}\right) + e_2\left(\frac{\dot{m}}{\dot{m}_{max}}\right)^2$
Heat dissipation	$\dot{Q}_{diss} = \frac{\dot{m}}{\rho}\left(\lvert\Delta p\rvert\left(\frac{1}{\eta} - 1\right) + aL\dot{m}^2\right)$
Power consumption	$W = \frac{\frac{\dot{m}}{\rho}\ \lvert\Delta p\rvert}{\eta}$
Heat loss	$\dot{Q}_{loss} = UA\,L\,(T - T_{ext})$

- d pump direction, 1 if from node(in) to node(out), -1 if from node(out) to node(in)
- Δp_{max} hydraulic head with zero mass flow rate
- $\dot{m}_{max}$ mass flow rate with zero hydraulic head
- k_1 first-order coefficient of the normalized hydraulic curve
- e_0 zero-order coefficient of the efficiency curve
- e_1 first-order coefficient of the efficiency curve
- e_2 second-order coefficient of the efficiency curve
- a quadratic pressure drop coefficient per unit length
- UA UA value of pipe per unit length
- L element length
- T_{ext} external temeprature

Pipe

Momentum	$p_{out} - p_{in} = \Delta p - a\,L\,\lvert\dot{m}\rvert\dot{m}$
Heat dissipation	$\dot{Q}_{diss} = \frac{\dot{m}}{\rho}\left(\lvert\Delta p\rvert\left(\frac{1}{\eta} - 1\right) + aL\dot{m}^2\right)$
Heat loss	$\dot{Q}_{loss} = UA\,L\,(T - T_{ext})$

- a quadratic pressure drop coefficient per unit length
- UA UA value of pipe per unit length
- L element length
- T_{ext} external temeprature

Substation (with assigned thermal load and secondary circuit temperatures)

Heat dissipation	$\dot{Q}_{diss} = \frac{\dot{m}}{\rho}\left(\lvert\Delta p\rvert\left(\frac{1}{\eta} - 1\right) + aL\dot{m}^2\right)$
Return temperature	$\frac{[(T_{s1} - T_{s2}) - (T_{r1} - T_{r2})]}{ln\left(\frac{T_{s1} - T_{s2}}{T_{r1} - T_{r2}}\right)} = \frac{\dot{Q}_{user}}{UA_{HX}}$
Flowrate	$\dot{m} = \min\left(\dot{m}_{max}, \frac{\dot{Q}_{user}}{[c_p(T_{s1} - T_{r1})]}\right)$

- $\dot{Q}_{user}$ thermal load (positive for heating)
- L element length
- UA_{HX} heat exchanger UA value
- T_{ext} external temeprature
- T_{s1}, T_{r1} supply and return temperature on the primary side of the heat exchanger
- T_{s2}, T_{r2} supply and return temperature on the secondary side of the heat exchanger
- $\dot{m}_{max}$ maximum (design) mass flow rate

Generator with constant outlet temperature

Momentum	$p_{out} - p_{in} = \Delta p - a\,L\,\lvert\dot{m}\rvert\dot{m}$
Heat dissipation	$\dot{Q}_{diss} = \frac{\dot{m}}{\rho}\left(\lvert\Delta p\rvert\left(\frac{1}{\eta} - 1\right) + aL\dot{m}^2\right)$
Heat generation	$\dot{Q}_{gen} = \lvert\dot{m}\rvert c_p(T_{set} - T_{in}) - \dot{Q}_{diss}$

- a quadratic pressure drop coefficient per unit length
- L element length
- T_{set} outlet temperature set point

References

[1] European union, directive 2012/27. EU on energy efficiency; 2012.
[2] European commission, communication COM(2016) 51 final. An EU Strategy on Heating and Cooling; 2016.
[3] Brange L, Englund J, Lauenburg P. Prosumers in district heating networks - a Swedish case study. Appl Energy 2016;164:492–500. https://doi.org/10.1016/j.apenergy.2015.12.020.
[4] De Uribarri PMÁ, Eicker U, Robinson D. Energy performance of decentralized solar thermal feed-in to district heating networks. Energy Procedia; 2017. p. 285–96. https://doi.org/10.1016/j.egypro.2017.05.075.
[5] Di Pietra B, Zanghirella F, Puglisi G. An evaluation of distributed solar thermal "net metering" in small-scale district heating systems. Energy Procedia; 2015. p. 1859–64. https://doi.org/10.1016/j.egypro.2015.11.335.
[6] Brand L, Calvén A, Englund J, Landersjö H, Lauenburg P. Smart district heating networks - a simulation study of prosumers' impact on technical parameters in distribution networks. Appl Energy 2014;129:39–48. https://doi.org/10.1016/j.apenergy.2014.04.079.
[7] Buffa S, Cozzini M, D'Antoni M, Baratieri M, Fedrizzi R. 5th generation district heating and cooling systems: a review of existing cases in Europe. Renew Sustain Energy Rev 2019;104:504–22. https://doi.org/10.1016/j.rser.2018.12.059.
[8] Lund H, Duic N, Østergaard PA, Mathiesen BV. Future district heating systems and technologies: on the role of smart energy systems and 4th generation district heating. Energy 2018;165:614–9. https://doi.org/10.1016/j.energy.2018.09.115.
[9] Lund H, Østergaard PA, Nielsen TB, Werner S, Thorsen JE, Gudmundsson O, Arabkoohsar A, Mathiesen BV. Perspectives on fourth and fifth generation district heating. Energy 2021;227:120520. https://doi.org/10.1016/j.energy.2021.120520.
[10] Dénarié A, Aprile M, Motta M. Heat transmission over long pipes: new model for fast and accurate district heating simulations. Energy 2019;166:267–76. https://doi.org/10.1016/J.ENERGY.2018.09.186.
[11] Benonysson A. Dynamic modelling and operation optimization of district heating systems. PhD Thesis. Denmark: Technical University of Denmark (DTU); 1991.
[12] Dancker J, Wolter M. Improved quasi-steady-state power flow calculation for district heating systems: a coupled Newton-Raphson approach. Appl Energy 2021;295:116930. https://doi.org/10.1016/j.apenergy.2021.116930.
[13] Stevanovic VD, Prica S, Maslovaric B, Zivkovic B, Nikodijevic S. Efficient numerical method for district heating system hydraulics. Energy Convers Manag 2007;48:1536–43. https://doi.org/10.1016/j.enconman.2006.11.018.
[14] Wang Y, Wang X, Zheng L, Gao X, Wang Z, You S, Zhang H, Wei S. Thermo-hydraulic coupled analysis of long-distance district heating systems based on a fully-dynamic model. Appl Therm Eng 2023;222:119912. https://doi.org/10.1016/j.applthermaleng.2022.119912.
[15] Ben Hassine I, Eicker U. Impact of load structure variation and solar thermal energy integration on an existing district heating network. Appl Therm Eng 2013;50:1437–46. https://doi.org/10.1016/j.applthermaleng.2011.12.037.
[16] Guelpa E, Sciacovelli A, Verda V. Thermo-fluid dynamic model of large district heating networks for the analysis of primary energy savings. Energy 2019;184:34–44. https://doi.org/10.1016/j.energy.2017.07.177.
[17] Vivian J, Quaggiotto D, Zarrella A. Increasing the energy flexibility of existing district heating networks through flow rate variations. Appl Energy 2020;275:115411. https://doi.org/10.1016/j.apenergy.2020.115411.
[18] Vesterlund M, Dahl J. A method for the simulation and optimization of district heating systems with meshed networks. Energy Convers Manag 2015;89:555–67. https://doi.org/10.1016/j.enconman.2014.10.002.
[19] Sartor K, Thomas D, Dewallef P. A comparative study for simulating heat transport in large district heating networks. In: ECOS 2015 Int. Conf. France: Pau; 2015.
[20] V Larsen H, Bøhm B, Wigbels M. A comparison of aggregated models for simulation and operational optimisation of district heating networks. Energy Convers Manag 2004;45:1119–39. https://doi.org/10.1016/j.enconman.2003.08.006.
[21] Pálsson H. Methods for planning and operating decentralised combined heat and power plants. PhD Thesis. Roskilde, Danemark: Riso National Laboratory; 2000.
[22] Dalla Rosa A, Li H, Svendsen S. Method for optimal design of pipes for low-energy district heating, with focus on heat losses. Energy 2011;36:2407–18. https://doi.org/10.1016/j.energy.2011.01.024.
[23] Dalla Rosa A, Li H, Svendsen S. Modeling transient heat transfer in small-size twin pipes for end-user connections to low- energy district heating networks. Heat Transf. Eng. ISSN. 2013;34:372–84. https://doi.org/10.1080/01457632.2013.717048.
[24] Gabrielaitiene I, Bøhm B, Sunden B. Evaluation of approaches for modeling temperature wave propagation in district heating pipelines. Heat Tran Eng 2008;29:45–56. https://doi.org/10.1080/01457630701677130.
[25] Gabrielaitiene I. Numerical simulation of a district heating system with emphases on transient temperature behaviour. Vilnius: 8th Int. Conf. Environ. Eng.; 2011. p. 747–54.
[26] Gabrielaitienė I, Bøhm B, Sundén B. Dynamic temperature simulation in district heating systems in Denmark regarding pronounced transient behaviour. J Civ Eng Manag 2011;17:79–87. https://doi.org/10.3846/13923730.2011.553936.
[27] Gabrielaitiene I, Sunden B, Bøhm B, Larsen H. Dynamic performance of district heating system in Madumvej, Denmark. In: 10th Int. Symp. Dist. Heat. Hanover: . Cool.; 2006.
[28] Gabrielaitiene I, Bøhm B, Sunden B. Modelling temperature dynamics of a district heating system in Naestved, Denmark—a case study. Energy Convers Manag 2007;48:78–86. https://doi.org/10.1016/j.enconman.2006.05.011.
[29] of Wisconsin-Madison SELU. TRNSYS 16 Mathematical Reference 2006. https://doi.org/10.1108/978-1-78743-527-820181015.
[30] Oppelt T, Urbaneck T, Gross U, Platzer B. Dynamic thermo-hydraulic model of district cooling networks. Appl Therm Eng 2016. https://doi.org/10.1016/j.applthermaleng.2016.03.168.
[31] Maurer J, Ratzel OM, Malan AJ, Hohmann S. Comparison of discrete dynamic pipeline models for operational optimization of District Heating Networks. Energy Rep 2021;7:244–53. https://doi.org/10.1016/j.egyr.2021.08.150.
[32] Meibodi SS, Rees S. Dynamic thermal response modelling of turbulent fluid flow through pipelines with heat losses. Int. J. Heat Mass Transf. 2020;151:119440. https://doi.org/10.1016/j.ijheatmasstransfer.2020.119440.
[33] Barone G, Buonomano A, Forzano C, Palombo A. A novel dynamic simulation model for the thermo-economic analysis and optimisation of district heating systems. Energy Convers Manag 2020;220:113052. https://doi.org/10.1016/j.enconman.2020.113052.
[34] Steinegger J, Wallner S, Greiml M, Kienberger T. A new quasi-dynamic load flow calculation for district heating networks. Energy 2023;266:126410. https://doi.org/10.1016/j.energy.2022.126410.
[35] Giraud L, Baviere R, Vallée M, Paulus C. Presentation, validation and application of the district heating Modelica library. Proc. 11th Model. Conf. 2015:79–88. https://doi.org/10.3384/ecp1511879.
[36] Van Der Heijde B, Fuchs M, Tugores CR, Schweiger G, Sartor K, Basciotti D, Müller D, Nytsch-Geusen C, Wetter M, Helsen L. Dynamic equation-based thermo-hydraulic pipe model for district heating and cooling systems. Energy Convers Manag 2017;151:158–69. https://doi.org/10.1016/j.enconman.2017.08.072.
[37] Python, (n.d.). https://www.python.org/.

[38] Röder J, Meyer B, Krien U, Zimmermann J, Stührmann T, Zondervan E. Optimal design of district heating networks with distributed thermal energy storages – method and case study. Int. J. Sustain. Energy Plan. Manag. 2021;31:5–22. https://doi.org/10.5278/ijsepm.6248.
[39] Oemof community, DHNx, (n.d.). https://github.com/oemof/DHNx.
[40] Oemof community, Oemof, (n.d.). https://github.com/oemof/.
[41] Vorspel L, Bücker J. District-heating-grid simulation in python: digripy. Computation 2021;9. https://doi.org/10.3390/computation9060072.
[42] Witte F, Tuschy I. TESPy: thermal engineering systems in Python. J Open Source Softw 2020;5:2178. https://doi.org/10.21105/joss.02178.
[43] Sartor K, Dewalef P. Experimental validation of heat transport modelling in district heating networks. Energy 2017;137:961–8. https://doi.org/10.1016/j.energy.2017.02.161.
[44] Kozen DC. Depth-first and breadth-first Search. In: Des. Anal. Algorithms. Texts Monogr. Comput. Sci. New York, NY: Springer; 1992. p. 19–24. https://doi.org/10.1007/978-1-4612-4400-4_4.
[45] Lax PD. Hyperbolic systems of conservation laws and the mathematical theory of shock waves. Society for Industrial and Applied Mathematics; 1973. https://doi.org/10.1137/1.9781611970562.ch1.
[46] Lienhard JH, IV JH, Lienhard V. A heat tranfer textbook. fourth ed. Cambridge, MA: Phlogiston Press; 2017.
[47] Toro FE. Riemann solvers and numerical methods for fluid dynamics. Berlin, Heidelberg: Springer; 1999.
[48] AIRU. Il riscaldamento urbano - annuario 2013. Milano: Tecnedit; 2013.